Reduction of attenuation correction artifacts in PET-CT

Johan Nuyts, Sigrid Stroobants

Abstract— **The conventional approach to attenuation correction in PET-CT, is to derive an attenuation map from the reconstructed high resolution CT image. For that purpose, the CT image is resampled to a lower resolution, the CT-values are converted to attenuation coefficients at 511 keV, and the resulting image is projected to generate the attenuation correction sinograms. In the approach followed here, the PET attenuation image is computed from the raw CT data rather than from the clinical CT-image. The CT data are first reduced to PET resolution and rebinned into parallel hole geometry. This reduced data set can be reconstructed with iterative algorithms in reasonable processing times. Existing algorithms have been combined into a procedure that generates attenuation maps in which the artifacts due to metal implants, oral and intravenous contrasts agents have been reduced.**

The procedure combines the "projection completion" method with maximum-likelihood reconstruction to suppress metal artifacts. The first evaluation in patients reveals excellent performance.

To suppress the influence of intravenous contrast, attenuation values higher than that of water were simply replaced with the attenuation of water. This method was evaluated in seven patient PET-CT studies, each of them consisting of two CT-scans and one PET-scan. One CT scan was acquired before, the other one after administration of the intravenous contrast agent. In these 7 patients, 18 volumes of interest were studied. With the conventional method, the mean difference in standardized uptake value (SUV) produced with the two CT-scans was 3.3%, with a maximum of 11.5%. With the alternative conversion method, this difference was reduced to 1.5%, with a maximum of 8.5%. The comparison of the two CTs also revealed differences due to tissue and patient motion. The SUVs seem to be more affected by this motion than by the IV-contrast.

I. Introduction

CT-based attenuation correction in PET-CT is much faster and introduces far less noise than the attenuation correction based on transmission scans in stand alone PET systems. However, the sensitivity of the CT to dense materials such as metal implants, and the conversion from CT Hounsfield units to PET attenuation correction factors can produce artifacts. The traditional approach is to start from the (diagnostic) CT image and derive an attenuation map with reduced resolution. Here, we propose to first reduce the resolution of the raw CT data to that of PET. This results in a strong reduction of the sinogram size, enabling application of iterative reconstruction in a clinically acceptable processing time.

II. Method

The procedure proposed here consists of a combination of existing methods.

Nuclear Medicine, K.U.Leuven, B-3000 Leuven, Belgium. (e-mail: Johan.Nuyts@uz.kuleuven.be and Sigrid.Stroobants@uz.kuleuven.be)

First, the CT sinogram is resampled to the PET detector size and rebinned from fan beam to parallel beam configuration. The method is implemented for a dual slice CT and helical acquisition orbit: linear interpolation is used to produce sinograms for axial positions exactly matching that of the PET slices. A CT-image is then reconstructed using a maximum-likelihood algorithm for transmission tomography [1], [2], called "MLTR" in the rest of this paper. The "raw" CT data obtained from the scanner have actually undergone several corrections, including the log-conversion, converting the measured intensities to the integrals of attenuation coefficients. The MLTR algorithm starts from a blank and a transmission sinogram, assuming that the blank sinogram is noise-free, while the transmission sinogram values are samples from a Poisson distribution. Although the real distribution is not exactly Poisson, the approximation is reasonable, and rightly assigns a lower certainty to values corresponding to higher attenuation. In order to apply MLTR to the CT-data, an arbitrary noise-free blank scan of 10^5 photons per detector pixels is introduced. The transmission scan is calculated as $t_i = b_i \exp(-r_i)$, where b_i is the blank scan value for detector element i, r_i is the "raw" CT-value and t_i the computed transmission value.

In the presence of metal prostheses, MLTR will still produce artifacts, unless the energy spectrum of the tube is accurately modeled and partial volume effects are avoided in the projector and backprojector. Algorithms for polychromatic transmission sources have been developed [3], [4], but they require relatively long computation times. To reduce the computation time, and to avoid problems with partial volume effects, MLTR was combined here with a so-called projection completion method [5], [6]. First the image is reconstructed with MLTR (100 iterations accelerated with subsets). The resulting image is thresholded using a threshold of 0.5 cm^{-1}. If there are no values exceeding the threshold, it is assumed that there are no metal artifacts and the reconstruction is considered complete. Otherwise, a binary image of the metal is produced by setting the pixels exceeding the threshold to 1 and all other pixels to zero. This image is projected to produce a "footprint" of the metal in the sinogram. A mask for the sinogram is defined as the set of all pixels where the footprint is non-zero. All pixel values within the mask are considered unreliable. The CT-projection is then "completed" by replacing the pixel values within the mask by interpolated values: linear interpolation between the nearest pixels outside the mask was used. Finally, the footprint multiplied with an arbitrary density D is added to the interpolated sinogram. Consequently, the unreliable measured projection of the metal is replaced by a computed

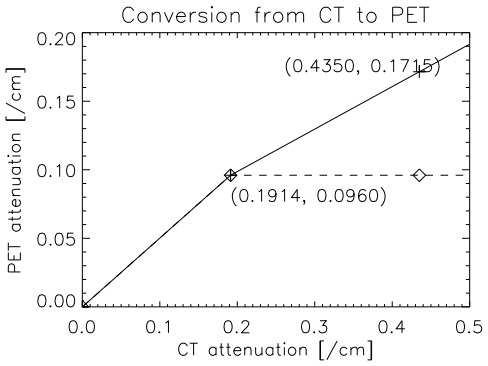

Fig. 1. Conversion from CT to PET attenuation: hybrid method (solid line) and clipping method (dashed line).

projection of an object of a similar shape with a density that is D higher than that of the surrounding tissues. This modified projection is then again reconstructed with MLTR. With this approach, the metal is still visible as a structure with the appropriate shape and increased density. Moreover, MLTR should still assign lower weights to the computed projections (due to the higher density), which is expected to be beneficial, because projection completion with linear interpolation is an approximate method, expected to introduce inconsistencies. However, we found that with a very high value for D, the inversion problem becomes more ill-posed, resulting in slower convergence and appearance of streak artifacts. Good results were obtained with a value $D = 0.22$ cm^{-1}, but the effect of D on streak artifact reduction remains to be investigated.

Next, the CT values have to be converted to PET attenuation values. The current standard is the so-called hybrid method [7], which has shown to be effective in absence of contrast agents. However, it produces an inappropriate scaling of contrast enhanced regions. Following the suggestion of several researchers, we use the scaling of Kinahan et al [7] for regions less dense than tissue, while the contrast artifacts are suppressed by simply setting the attenuation of denser regions to that of tissue. This approach is similar to that of Lonn [8] and causes undercorrection for bone attenuation, but strongly reduces contrast related artifacts. For many tracers, including ^{18}F-FDG, the uptake in bone is very low, and the undercorrection of bone attenuation is not expected to produce noticeable artifacts. For the hybrid method, a piecewise linear scaling curve was used, converting CT attenuation values (unit is cm^{-1}) from [0, 0.1914, 0.435] to [0, 0.096, 0.1715] as illustrated in fig. 1. The alternative conversion method, called the "clipping method", simply sets all values higher than 0.096 cm^{-1} to 0.096 cm^{-1} (fig 1).

Finally, the resulting image is forward projected to produce the attenuation correction sinogram. For comparison, the conventional method was simulated by reconstructing the CT with FBP and applying the hybrid method. We verified that the resulting PET images were similar to the clinical images obtained with the commercial software.

III. Patient studies

All PET-CT images were acquired on a Biograph system (Siemens), consisting of a dual slice CT system (Somatom Emotion) and a septaless LSO PET camera (Ecat Accel). The CT data were acquired with a slice thickness of 5 mm, using a 12 mm table feed per rotation, with a rotation time of 0.8 s. Low dose CT scans were acquired at 40 mAs and 110 kVp, full diagnostic CT scans were acquired at 85 mAs and 130 kVp. The PET acquisition was done with 4 minutes per bed position, with typically 7 bed positions per study. The performance characteristics of the PET-system have been published by Herzog et al [9].

As described previously, the raw CT data were copied from the PET-CT system for off-line reconstruction. The CT-reconstruction was described in the previous section. To generate attenuation maps, the rescaled CT-images were projected into 3D attenuation correction sinograms. The 3D PET sinograms then were corrected for detector sensitivity, dead time and attenuation, and converted to 2D sinograms with Fourier rebinning [10]. For reconstruction, the sinograms were "uncorrected" for attenuation, and reconstructed with (attenuation weighted) MLEM, accelerated using a gradually decreasing number of subsets.

For comparison, the PET images were also reconstructed without attenuation correction, using a maximum-likelihood algorithm that allows negative values in the reconstruction [11]. This algorithm avoids loss of visual information due to the nonnegative constraint of standard MLEM.

A. Metal streak artifacts

Two PET-CT patient studies were selected to evaluate the performance of streak artifact suppression in the presence of very dense objects. The first patient had a large spine prosthesis and was referred to investigate possible infection near the prosthesis. The second patient underwent a PET-CT scan for staging of oesophageal cancer. He had previously undergone a barium swallow examination with persistent barium residues in the colon at the day of the PET-CT examination. This barium contrast agent is sufficiently dense to produce severe streak artifacts in the CT images.

B. Intravenous contrast

To evaluate the more subtle influence of intravenous contrast on the quantitative analysis of PET images, the baseline PET-CT scans of cancer patients included in a phase II trial evaluating the efficacy of a histone deacetylase inhibitor were analyzed. The imaging protocol for this project involves the acquisition of two whole body CT scans and one whole body PET scan. First a low dose CT scan is acquired for attenuation correction unaffected by intravenous contrast. This is followed by the PET scan, which takes about 30 min. Finally a full diagnostic CT with IV contrast containing 300 mg iodine per ml is performed. For the analysis of the PET images, volumes-of-interest (VOI) are delineated by the physicians, using software based on thresholding and region growing [12], and the mean SUV of the VOI is computed.

To quantify to what extent intravenous contrast would affect this medical research study, the scans are reprocessed and the SUVs in these same VOIs are recomputed. The reprocessing involves four different ways of computing the attenuation correction sinograms, each of them generating a different attenuation corrected PET image. These PET images are obviously exactly matched, such that VOIs defined on one image can be applied immediately to the other images. The four attenuation correction procedures are:

1) *conventional without contrast:* the low dose CT is reconstructed with FBP and converted with the hybrid method.
2) *conventional with contrast:* same procedure applied to the full diagnostic CT
3) *new procedure without contrast:* the low dose CT is reconstructed with MLTR with projection completion and converted with the clipping method.
4) *new procedure with contrast:* same procedure applied to the full diagnostic CT.

This study reports on the results obtained by reprocessing 7 patient studies, yielding results for 18 VOIs.

IV. Results

A. Suppression of streak artifacts

The method was applied to a patient with a large prosthesis supporting the spine, as shown in fig. 2. This patient was also unable to raise the arms out of the field of view. Both the conventional CT image and the CT image obtained with the proposed method are shown in the figure, together with the corresponding attenuation corrected PET images. The PET image without attenuation correction is shown as well. The PET image produced with the new method agrees well with the image without attenuation correction. In contrast, the conventional PET image shows regions of increased tracer uptake near the prosthesis. The obvious disagreement with the non-attenuation corrected image indicates that these are artifacts. Figure 3 displays transaxial images of the two CTs, illustrating that MLTR eliminates the truncation artifacts near the arms, and, in combination with projection completion, strongly suppresses the artifacts due to the metallic implant.

Fig 4 illustrates the method applied to a patient scan with barium contrast residues in the colon from an earlier X-ray swallow examination of the digestive tract. MLTR with projection completion virtually eliminates the streak artifacts. The subsequent conversion method erases the contrast. The PET image without attenuation correction reveals that there is a lesion in the liver suspected for liver metastasis. The lesion is obscured by the contrast artifacts when the conventional attenuation correction method is used. With the proposed method, the artifact is suppressed and the liver metastasis is clearly visible. Again, good agreement with the non attenuation corrected image is obtained. Nehmeh et al [13] found that even when yielding a Hounsfield unit of 3000, $BaSO_4$ contrast produced only a small increase of the attenuation at 511 keV. This suggests that the artifact suppression may also have restored quantitative accuracy, because the computed attenuation map (image C in fig 4) is expected to be close to the true attenuation. This could not be verified because there was no gold standard in this patient study.

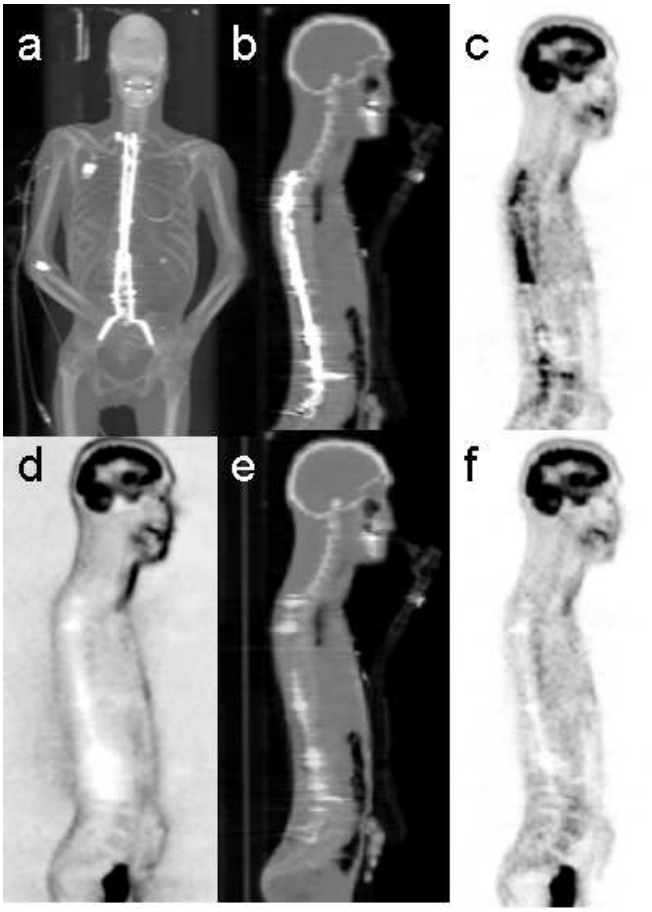

Fig. 2. PET-CT study, with **a)** a maximum intensity projection of the CT, and sagittal images of: **d)** PET image without attenuation; **b)** the conventional CT image and **c)** the corresponding PET image; **e)** the CT image obtained with MLTR + projection completion and **f)** the corresponding PET image.

Fig. 3. Metal artifact reduction with projection completion and maximum-likelihood reconstruction: FBP (left) and the proposed method (right)

B. Intravenous contrast

Figure 5 shows the difference between the CTs with and without contrast, obtained in the same patient. The difference between the CT-images not only shows the contrast enhancement, it also reveals many differences due to tissue motion between the scans. All these differences result in different apparent tracer uptake in the corresponding PET images. Figure 6 plots the relative differences between the computed SUV values, using the CT without IV-contrast (CT1) and conventional processing as the reference. Most SUVs

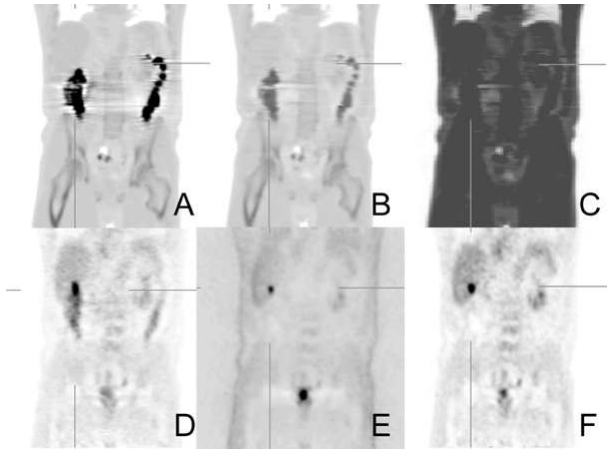

Fig. 4. Reduction of barium contrast artifacts. A: FBP of CT. B: projection completion and maximum-likelihood reconstruction. C: PET attenuation values. D: PET image, corrected with the hybrid method applied to A. E: PET image without attenuation correction. F: PET image corrected with C.

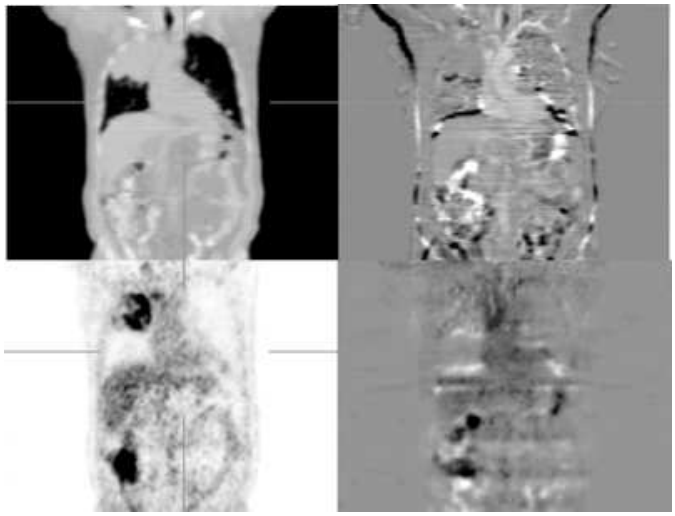

Fig. 5. Coronal slices through the CT without IV-contrast and the corresponding PET scan are shown at the left. The top right panel shows the difference between the two CT images (with and without contrast). The lower right image is the difference between the PET reconstructions obtained with attenuation correction based on each of the CTs.

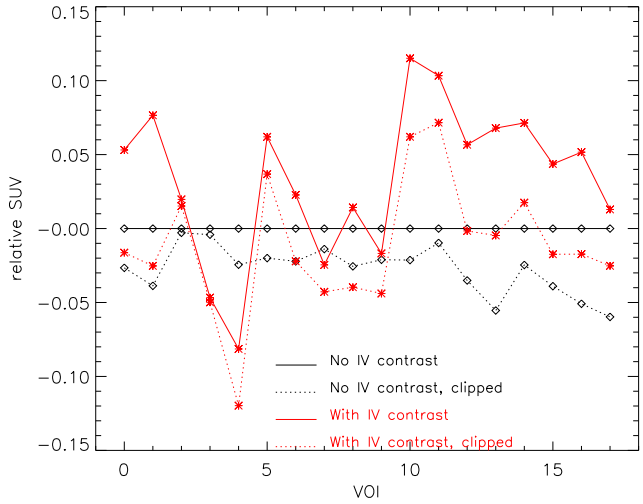

Fig. 6. The relative difference of the computed SUV for each of the 18 VOIs, using the first CT with conventional processing as the reference. Diamonds correspond to the first CT, asterisks to the second. Solid lines are used for the hybrid conversion method, dashed lines for the clipping method.

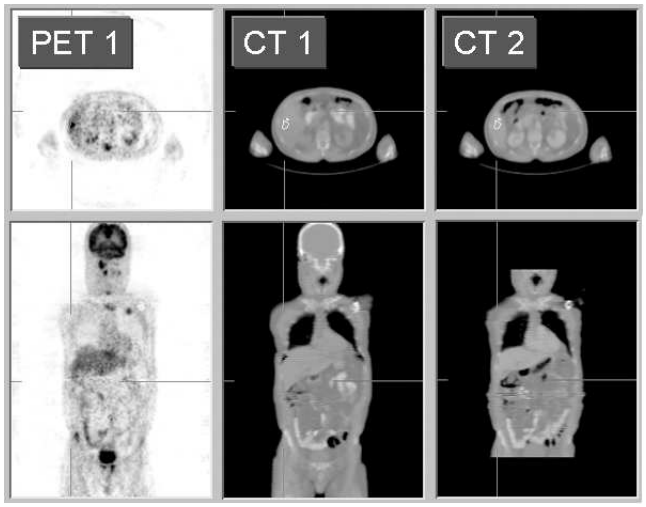

Fig. 7. VOI 4 (see fig. 6)

increase when the second CT (CT2) was used instead. When the clipping method is used instead of the hybrid method, the SUVs decrease, but more so for CT2.

With the hybrid method, the mean SUV increased with 3.3% when CT2 was used instead of CT1. The standard deviation of these SUV changes was 6.0%, and the maximum increase was 11.5%. For the clipping method, using CT2 increased the mean SUV with 1.5%, the standard deviation was 4.7% and the maximum increase was 8.5%. However, using CT1 (without IV-contrast) for attenuation correction, the mean SUV decreased with 2.8% (standard deviation 3.2%, maximum decrease of 6.3%) when clipping was used instead of the hybrid method. Apparently, the clipping method reduces the sensitivity to IV-contrast, but introduces negative bias. The clipping method yielded only a moderate decrease of the variance, indicating that there are other sources of variability than the IV-contrast.

C. Motion artifacts

As suggested by fig. 5 and by the numbers given in the previous section, IV-contrast is not the only source of variability. We closely examined VOI 4, a liver metastasis localized near the colon: its SUV (fig. 6) decreased when CT2 was used, while an increase was expected. As illustrated in fig 7, this is probably caused by the increased amount of air in the colon near the liver metastasis. The corresponding decreased attenuation correction apparently more than cancels the increased attenuation due to the IV-contrast.

V. Discussion

Metal artifacts in the CT image can severely distort the attenuation corrected PET images, making these images effectively useless. In these cases, the PET images without attenuation correction have to be used. The combination of maximum likelihood reconstruction with projection completion was shown

to be very effective in suppressing these artifacts. Visual quality is essentially restored, the effect on quantification remains to be studied. By resampling the raw CT data to PET resolution, the maximum likelihood reconstruction of the attenuation map can be done in clinically acceptable times. The required computation time is less than that of the emission reconstruction, because the latter are acquired in 3D mode (without septa), while resampling the CT data produces 2D sinograms.

The imaging protocol used to analyze the effect of intravenous contrast was similar to the one recently analyzed by Berthelsen et al. [14]. That study yielded similar findings: IV-contrast is only one of several causes of variability, the observed changes are usually in the order of a few percent with a maximum of about 10%, and are not expected to affect detection and staging. However when PET is used as a surrogate marker of response in early clinical trial, a reduction in FDG uptake of 15% after 1 cycle or 25% after 2 or more cycles is considered a partial response [15]. Therefore, the observed changes cannot be considered negligible in this setting. For that reason, every method that contributes to reducing this variation deserves attention.

The quantitative analysis indicates that the clipping method reduces the variance at the cost of increased bias. This may be beneficial for follow-up studies, where systematic errors are less important because the analysis is focused on changes in tracer uptake. It is possible that the method could be somewhat improved by optimizing the threshold value used for clipping. In this study, the threshold was set to the density of water. Inspection of the CT-images without IV-contrast revealed that many organs have actually a slightly lower density. It follows that lowering the threshold might yield a further reduction of the variability, at the cost of a further increase of negative bias. The clipping method studied here is very similar to the scaling method of Lonn [8]. It sacrifices accurate correction for bone attenuation, to suppress the influence of IV-contrast. Ignoring bone is expected to yield only a small negative bias because the normal FDG uptake in bone is low. However, in the case of bone metastases, the bias may be higher than what was observed in our study. Even in that case the method could be valuable for patient follow-up, because as argued above, (position dependent) negative bias is acceptable, as long as it does not change during the course of the follow-up period.

VI. Acknowledgment

The authors thank Michel Defrise and Xian Liu for the Fourier rebinning software, Christian Michel and Mérence Sibomana for scatter correction and file I/O software and Karl Stierstorfer and colleagues from Siemens for help with the CT file format.

References

[1] J Nuyts, B De Man, P Dupont, M Defrise, P Suetens, L Mortelmans. "Iterative reconstruction for helical CT: a simulation study." *Phys Med Biol,* 1998; 43: 729-737.

[2] B De Man, J Nuyts, P. Dupont et al. "Reduction of metal streak artifacts in x-ray computed tomography using a transmission maximum a posteriori algorithm", *IEEE Trans Nucl Sci*, 2000; 47 (3): 977-981.

[3] B De Man, J Nuyts, P Dupont, G Marchal, P Suetens. "An iterative maximum-likelihood polychromatic algorithm for CT". *IEEE Trans Med Imaging,* 2001; 20 (10): 999-1008.

[4] IA Elbakri, JA Fessler. "Segmentation-free statistical image reconstruction for polyenergetic x-ray computed tomography with experimental validation". *Phys Med Biol* 2003; 48: 2453-2477.

[5] RM Lewitt, RH Bates. "Image reconstruction from projections: III: Projection completion methods (theory)", *Optik*, vol. 50, 1978, pp. 189-204.

[6] WA Kalender, R Hebel, J Ebersberger. "Reduction of CT artifacts caused by metallic implants." *Radiology*, 1987: 164: 576-577.

[7] P Kinahan, D Townsend et al, "Attenuation correction for a combined 3D PET/CT scanner". *Med Phys* 1998; 25: 2046-2053.

[8] A Lonn. "Evaluation of method to minimize the effect of X-ray contrast in PET-CT attenuation correction". *IEEE NSS-MIC*, proceeding, 2003; vol 3, 2220-2221.

[9] H Herzog, L Tellmann, C Hocke, U Pietrzyk, ME Casey, T Kuwert. "NEMA NU2-2001 guided performance evaluation of four Siemens ECAT PET scanners" *IEEE Trans Nucl Sci*, 2004; 51: 2662-2669.

[10] M Defrise, PE Kinahan, DW Townsend, C Michel, M Sibomana, DF Newport. "Exact and approximate rebinning algorithms for 3-D PET data." *IEEE Trans Med Imaging,* 1997, 16: 145-158.

[11] J Nuyts, S Stroobants, P Dupont, S Vleugels, P Flamen, L Mortelmans. "Reducing loss of image quality due to the attenuation artifact in uncorrected PET whole body images." *J Nucl Med,* 2002; 43: 1054-1062.

[12] NC Krak, R Boellaard, OS Hoekstra, JWR Twisk, CJ Hoekstra, AA Lammertsma. "Effects of ROI definition and reconstruction method on quantitative outcome and applicability in a response monitoring trial", *Eur J Nucl Med Mol Imaging*, 2005; 32: 294 - 301, and 2005; 32: 1245.

[13] SA Nehmeh, YE Erid, H Kalaigian, KS Kolbert, T Pan, H Yeung, O Squire, A Sinha, SM Larson, JL Humm. "Correction for oral contrast artifacts in CT attenuation-corrected PET images obtained by combined PET/CT." *J Nucl Med* 2003; 44: 1940-1944.

[14] AK Berthelsen, S Holm, A Loft, TL Klausen, F Andersen, L Højgaard. "PET/CT with intravenous contrast can be used for PET attenuation correction in cancer patients." *Eur J Nucl Med Mol Imaging,* 2005; 32: 1167 - 1175.

[15] H Young, R Baum, U Cremerius, K Herholz, O Hoekstra, AA Lammertsma, J Pruim, P Price. "Measurement of clinical and subclinical tumour response using [18F]-fluorodeoxyglucose and positron emission tomography: review and 1999 EORTC recommendations. European Organization for Research and Treatment of Cancer (EORTC) PET Study Group." *Eur J Cancer* 1999, 35(13):1773-1782.